DOI:
10.1016/j.jconrel.2018.04.047

Document Version
Peer reviewed version

Image guided thermosensitive liposomes for focused ultrasound drug delivery: Using NIRF labelled lipids and topotecan to visualise the effects of hyperthermia in tumours

Miguel N. Centelles, Michael Wright, Po-Wah So, Maral Amrahli, Xiao Yun Xu, Justin Stebbing, Andrew D. Miller, Wladyslaw Gedroyc, Maya Thanou

PII: S0168-3659(18)30247-5
DOI: doi:10.1016/j.jconrel.2018.04.047
Reference: COREL 9274

To appear in: *Journal of Controlled Release*

Received date: 9 October 2017
Revised date: 25 April 2018
Accepted date: 27 April 2018

Please cite this article as: Miguel N. Centelles, Michael Wright, Po-Wah So, Maral Amrahli, Xiao Yun Xu, Justin Stebbing, Andrew D. Miller, Wladyslaw Gedroyc, Maya Thanou , Image guided thermosensitive liposomes for focused ultrasound drug delivery: Using NIRF labelled lipids and topotecan to visualise the effects of hyperthermia in tumours. The address for the corresponding author was captured as affiliation for all authors. Please check if appropriate. Corel(2018), doi:10.1016/j.jconrel.2018.04.047

Image Guided Thermosensitive Liposomes for Focused Ultrasound Drug Delivery: Using NIRF labelled lipids and topotecan to visualise the effects of hyperthermia in tumours

Miguel N. Centelles[1,*], Michael Wright[1,*], Po-Wah So[2], Maral Amrahli[1], Xiao Yun Xu[3], Justin Stebbing[4], Andrew D. Miller[5], Wladyslaw Gedroyc[6], and Maya Thanou[1,†]

[1]School of Cancer and Pharmaceutical Sciences, King's College London, UK

[2]Biomedical Imaging and Spectroscopy, King's College London, UK

[3]Department of Chemical Engineering, Imperial College London, UK

[4]Department of Surgery and Cancer, Imperial College London, UK

[5]Global Acorn Ltd. Temple Road London, UK

[6]Department of Experimental Medicine, Imperial College London, UK

[*]These authors contributed equally to this work.

[†]Corresponding author: maya.thanou@kcl.ac.uk

Abstract

Image guided drug delivery using imageable thermosensitive liposomes (iTSLs) and high intensity focused ultrasound (FUS or HIFU) has attracted interest as a novel and non-invasive route to targeted delivery of anti-cancer therapeutics. FUS-induced hyperthermia is used as an externally applied 'trigger' for the release of a drug cargo from within thermosensitive drug carriers. It is suggested that sub-ablative hyperthermia significantly modifies the permeability of tumour vasculature and enhances nanoparticle uptake. Here we describe the preparation and use of magnetic resonance imaging (MRI) and near infrared fluorescence (NIRF) thermosensitive liposomes for imaging and tracking of biodistribution and drug release in a murine cancer model. We prepared iTSLs to encapsulate topotecan (Hycamtin®), a chemotherapeutic agent which when released in tumours can be monitored by an increase in its intrinsic drug fluorescence. FUS was applied using feedback via subcutaneously placed fine-wire thermocouples to maintain and monitor hyperthermic temperatures. iTSL accumulation was detected within tumours using NIRF imaging immediately after liposome administration. Mild FUS-induced hyperthermia (3 min at 42 ^{o}C, 30 min post *i.v.*) greatly enhanced iTSLs uptake. A co-localised enhancement of topotecan fluorescence emission was also observed immediately after application of FUS indicating rapid triggered drug release. The phenomena of increased iTSL accumulation and concomitant topotecan release appeared to be amplified by a second mild hyperthermia treatment applied one hour after the first. MRI *in vivo* also confirmed enhanced iTSLs uptake due to the FUS treatments. Our imaging results indicate the effects of hyperthermia on the uptake of carriers and drug. FUS-induced hyperthermia combined with real time imaging could be used as a tool for tumour targeted drug delivery.

Key words: Near infra-red fluorescence, MRI, imaging, focused ultrasound, liposomes, topotecan, localised drug delivery, cancer

Introduction

A key goal of cancer drug research is to develop improved methods for personalised chemotherapies delivering the right treatment, in the right place, at the right time. In an attempt to address this, a number of approaches combining imaging modalities with theranostic nanoparticles have emerged [1]. Different imaging techniques are routinely used in preclinical drug development as well as in the clinic, such as positron emission tomography (PET), single photon emission computed tomography (SPECT), magnetic resonance imaging (MRI) and recently developed Near Infra-Red Fluorescence (NIRF) techniques that image specific tumour-associated molecular targets in near real time [2, 3]. Such imaging capabilities are important tools for drug discovery, as it offers a non-invasive approach for improving the understanding of drug distribution and therapeutic effect in preclinical studies [4, 5].

There has been significant interest in the use of nanoparticles as carriers for anti-cancer drugs, with the aim of enhancing target specificity and/or reducing systemic toxicity [6]. In the case of Doxil®, the liposomal nanoparticles increases the tumour's doxorubicin concentration and reduce systemic toxicity [7].

Localised mild hyperthermia (< 43^{o}C) appears to be greatly beneficial for increasing nanoparticle concentration in tumours by enhancing local blood and interstitial fluid flow (reducing interstitial blood pressure) and promoting the uptake of nanoparticles up to about 400 nm in diameter [8, 9]. Mild hyperthermia has shown strong effects when combined with neo-adjuvant chemotherapy and radiotherapy in clinic, improving existing treatment protocols [10, 11]. The use of hyperthermia in the clinic has lead to the development of a new generation of liposomes. Thermo-sensitive liposomes (TSLs) were designed to overcome the problem of slow drug release from previous formulations [12]. Yatvin and Weinstein introduced first the concept of TSL [13, 14]. Needham and co-workers then introduced lysolipids as key component in TSLs designed for cancer therapy and evaluated the impact of lipid mesophase transitions on small-molecule drug release [15]. Doxorubicin-enclosing TSL (e.g. Thermodox®) in combination with hyperthermia were found to be significantly more effective than either free doxorubicin or Doxil® at reducing tumour growth in mice xenografts and canine tumours [16, 17]. Results from a Phase I study with Thermodox®[18] with escalating doses of Thermodox® with radiofrequency ablation (RFA) concluded that Thermodox® was safe at administered dose of 50 mg/m^2 in these conditions. Thermodox® in combination with RFA is being tested in clinical trials to treat hepatocellular carcinoma (OPTIMA study) and recurrent wall breast cancer (DIGNITY) [11, 19]. Recently published result from the HEAT study indicated that RFA + thermosensitive liposomal doxorubicin efficacy is improved when RFA dwell time for a solitary lesion $\geq$ 45min [20].

Focused Ultrasound (FUS) induces deep and localised hyperthermia in a controlled manner when MR thermometry is used [21]. Its application to enhance accumulation of nanoparticles in tumours and/or induce drug release from carriers, has been studied during the last years. Dromi *et al.* presented an early study on 'low temperature sensitive liposomes' and showed that FUS exposures resulted in a more rapid delivery of doxorubicin as well as significantly higher tumour concentrations, compared with TSLs alone or FUS with non-thermosensitive liposomes [12]. Later studies co-encapsulated doxorubicin and a chelated gadolinium MRI contrast agent (ProHance®) into TSLs, with the objective of using the later as a proxy to characterise drug release in phantoms and *in vivo* [22, 23]. In addition to studying the physical mechanism of drug release, different lipidic membrane compositions were evaluated in response to FUS induced hyperthermia. De Smet *et al.* compared these improved TSLs with older formulation (e.g, like Doxil) and concluded that the lipid composition plays an important role on colloidal stability and drug release profile [23]. The mechanism of cargo release with increased temperature appeared to result from the development of pores in the lipid membrane [24]. Other structure/activity correlations have been carried out since [25] and radiolabelling have also been integrated into TSL formulations alongside encapsulated MRI contrast agents to create bi-modal imaging systems [26] . Vaglianti *et al.* introduced $MnSO_4$/doxorubicin loaded liposomes to show that thermally-induced release significantly shortened T_1 suggesting that liposome contrast agents have the potential for use with hyperthermia by providing individualised monitoring of tissue drug concentration distribution during or after treatment [27]. In order to image their liposomes de Smet *et al.* introduced [$Gd(HPDO_3A)(H_2O)$] (ProHance®) within the core and confirmed drug release using MRI [28]. Thermosensitive liposome formulation parameters have been also investigated. Tagami *et al.* introduced thermosensitive liposomal formulation (HaT: Hyperthermia-activated-cytoToxic) consisting of DPPC and Brij78 (a surfactant) that showed enhanced drug delivery compared to lyso-lipid temperature sensitive liposomes (LTSL) [29] Ferrara's group discussed a version of TSLs carrying doxorubicin complexed with copper that appeared to show improved release properties, as assessed by hyperspectral optical imaging of intrinsic doxorubicin fluorescence [30]. Hijnen *et al.* prepared TSLs coencapsulating doxorubicin and ProHance to compare the effect of ablation in combination with hyperthermia in tumour bearing rats. The combination of hyperthermia-triggered drug delivery followed by ablation showed the best therapeutic outcome compared with other treatments. This appeared to be due to direct induction of thermal necrosis in the tumour core and efficient drug delivery to the surrounding rim [31].

Most recent studies indicate the importance of imaging when focused ultrasound and TSLs (LTSLs) are used for targeted drug delivery and are developed for translation to the clinic [11, 32, 33]. Our

aim is to use imaging to identify mechanisms of iTSLs (imaging TSLs) accumulation in tumours when hyperthermia protocols are applied and image the drug release in real time.

Previous work from our group has included proof-of-principle demonstrations of dual MRI/fluorescence labelled imaging liposomes with folate-receptor targeting for enhanced tumour cell uptake [34-39]. This involved the design, synthesis and early application of a novel *in vivo* compatible gadolinium lipid gadolinium (III) 2-(4,7-bis-carboxymethyl-10-[(*N*,*N*-distearyl-amidomethyl)-*N*`-amidomethyl]-1,4,7,10-tetraazacyclodo-dec-1-yl) acetic acid (Gd.DOTA.DSA; Scheme 1). Optical imaging or *in vivo* NIRF may be greatly improved (in terms of sensitivity and tissue penetration) by the use of fluorescence labels that absorb and emit in the 700-1000 nm 'window' [40]. In addition to the MRI labels we have developed a lipidic anchored NIRF label based on XenoLight 750 (Perkin Elmer, MA USA) which shows peak absorption at ~ 750 nm and extremely bright emission at 800 nm [41]. The brightness of this probe (XL750.DSA; *N*`-XenoLight750-*N*,*N*-distearylamidomethylamine) allows its inclusion at very low concentrations within the membrane of the liposomes (typically ~ 0.1 mol%), enabling labelling without apparently affecting their biophysically properties. Optical imaging may also be used to assess the release of liposomal drugs if there is sufficient difference in fluorescence properties between the encapsulated (low pH) and released states (high pH). Particularly well suited is the anti-cancer agent topotecan (Hycamtin®) which shows a significant shift in absorbance maxima (and hence fluorescence brightness) depending on pH. In our recent work, we prepared a LTSL topotecan-iTSLs labelled with NIRF-lipids for the purpose to understand iTSL biodistribution in mice [41]. In that work we used a thermosensitive liposomal formulation that included two labelled lipids and topotecan. Monitoring both lipids biodistribution we identified that these liposomes kept their composition and lipid mol% ratio on their way to tumours, and using a heating block on the tumour we induced topotecan release locally [41].

Here, we aim to understand and image the drug and/or liposomes' bio-distribution phenomena in tumours after brief application(s) of FUS. We prepared a novel formulation of bimodal iTSL labelled with both MRI and NIRF imaging agents, anchored to the lipid membrane allowing the tracking of the liposomes with both modalities. Our studies included developing this novel formulation for thermosensitivity and we assessed its potential of being activated using focused ultrasound *in vivo* in mice. The hypothesis is that by labelling the lipidic part of the iTSLs with a clinically relevant contrast agent, they can act as theranostic agents. Using MRI a clinical imaging modality here, we assess their biodistribution in tumours providing evidence that these iTSLs can be used with novel techniques such as MRI guided focused ultrasound. Their distribution into tumour lesions (primary and/or

metastatic) may be assessed in real time, before activating drug release by application of FUS-induced hyperthermia. We suggest that this real time imaging provides valuable feedback, allowing proper optimisation of FUS time points and periods to optimise the enhanced uptake effect. Imaging information coming from the topotecan fluorescence signal was also used here to assess and confirm drug release as induced by a small animal FUS system.

Materials and Methods

General Methods

1,2-Dipalmitoyl-*sn*-glycero-3-phosphocholine (DPPC; 16:0 PC), 1,2-distearoyl-*sn*-glycero-3-phosphocholine (DSPC; 18:0 PC), 1-stearoyl-*sn*-glycero-3-phosphocholine (MSPC; 18:0 Lyso PC) and (ω-methoxy-polyethylene glycol 2000)-*N*-carboxy-1,2-distearoyl-*sn*-glycero-3-phosphoethanolamine (PEG^{2000}-DSPE) were purchased from Sigma Aldrich (St. Louis, MO, USA) or Avanti Polar Lipids (Alabaster, AL, USA). DOTA-NHS-ester was purchased from Macrocyclics (Dallas, TX, USA) and XenoLight750-NHS-ester from Perkin Elmer (Waltham, MA, USA). Cell media were from Life Technologies (Carlsbad, CA, U.S.) while other materials were from Sigma-Aldrich and were of analytical grade. Other lipids were synthesised as described below.

^{1}H (400 MHz) and ^{13}C (100 MHz) NMR spectra were recorded on a Bruker Advance 400 spectrometer using residual chloroform or dichloromethane as internal standards. Results are reported as chemical shifts in ppm from TMS, with peaks described as s = singlet, br = broad singlet, d = doublet, t = triplet, q = quartet, m = multiplet, and coupling constants J given in hertz (Hz). Mass spectroscopy was carried out on a Thermo LCQ DECA XP or Agilent HP1100 MSD spectrometers depending on availability. Analytical HPLC was carried out using an Agilent 1100 series instrument equipped with a multi-wavelength diode array detector, a 1260 Infinity fluorescence detector, a Polymer Laboratories PL-ELS-2100 evaporative light scattering (ELS) detector, and a 5 cm Hypersil C18 5 µm reverse-phase column. For topotecan analysis, the HPLC was equipped with a cooled sample chamber (8-12 °C) and run as described in the pharmacokinetics section below. Synthesised lipids were analysed using gradient: 0 min, 100% water, 2.5 mL/min; 1 min, 100% water; 11 min, 100% MeCN; 11 min, 100% MeCN; 23 min, 100% methanol; 25 min, 100% methanol; 27 min, 100% water, 1.8 mL/min; 30 min, 100% water, 2.5 mL/min with primary detection by ELS and showed purity at least 95%. Thin Layer Chromatography (TLC) was carried out on F254 silica gel 60 plates, with spots visualised by UV illumination or vanillin/ninhydrin staining and developed with a heat gun. Flash column chromatography was performed on 40-63 µm silica gel.

Synthesis of lipids

Analytical characterisation data are shown in supplementary information.

***N*,*N*-Distearylamidomethylamine (DSA)** was synthesised according to Kamaly et al.

***N*`-XenoLight750-*N*,*N*-distearylamidomethylamine (XL750.DSA)**. DSA (4.2 mg; 7.3 µmol) was dissolved in dry DCM (0.2 mL) with distilled triethylamine (20 µL, 0.14 mmol). XenoLight750-NHS (1 µmol) dissolved in dry DMSO (100 µL; requires vigorous vortexing) was added, the flask protected from light and gently stirred. TLC (15 % methanol in CH_2Cl_2 with 0.5% NH_3) showed conversion of separate DSA (R_f 0.55) and XenoLight750-NHS (R_f 0.10) spots to a streak (R_f 0.40-0.65) over 5 h. The reaction was then stopped and dried *in vacuo* before purification by flash column chromatography (2 mL) loaded in CH_2Cl_2 and eluted with 5 % (DSA; colourless); 15-20 % (conjugate; blue; R_f 0.65); then 30 % (side product; colourless; R_f 0.45-0.55) MeOH with unconjugated dye retained on the column. The XL750-DSA fractions were combined and dried *in vacuo* to give a dark-blue solid with an estimated 70 % yield. This was dissolving to 1 mg/mL in chloroform and then stored at -20 ^{o}C.

Gadolinium (III) 2-(4,7-Bis-carboxymethyl-10-[(*N*, *N*-distearylamidomethyl-*N*'-amidomethyl]-1,4,7,10-tetraazacyclododec-1-yl) acetic acid (Gd.DOTA.DSA) was synthesised by adaption of the protocol of Kamaly *et al*. [34]. In brief, DOTA-NHS-ester (100 mg, 0.120 mmol) and DSA (80.2 mg, 0.139 mmol) were dissolved in dry CH_2Cl_2 (40 mL). Distilled Et_3N (67 µL, 0.48 mmol) was added and the mixture stirred under N_2 for 12 h at 35^{o}C. The solution was dried *in vacuo* and purified by flash chromatography loaded in 10 % CH_2Cl_2:MeOH:NH_2 (34.5:9:1) mixture in CH_2Cl_2 and eluted with increasing concentration to 100% of the solvent mixture. Fractions containing the target were identified by HPLC, combined and dried to give white hydroscopic solid (57.0 mg; 49 %). Gadolinium complexation was effected by suspension of DOTA-DSA (25.2 mg, 0.026 mmol) in a vigorously stirred aqueous solution (5 mL) of gadolinium (III) chloride hexahydrate (11.2 mg, 0.03 mmol) heated at 90 ^{o}C for 12 h under N_2. After settling, the excess water was removed and minimal CH_2Cl_2 added to dissolve the lipid complex. After vigorous mixing with equal amounts of deionised water, the emulsion was separated by centrifugation and the CH_2Cl_2 layer collected and dried *in vacuo* to give a white power (27 mg; 95%).

Formulation of topotecan-encapsulating liposomes

All lipids were stored in aliquots (10 mg/mL) in either $CHCl_3$ or MeOH/$CHCl_3$ 50:50 (v/v). Liposomes were prepared with the following lipid formations; Gd.DOTA.DSA/DPPC/DSPC/MSPC/PEG^{2000}-DSPE/XL750.DSA, 30:53.95:5:5:6:0.05 (mol%) for iTSL or DPPC/MSPC/PEG^{2000}-DSPE/XL750.DSA, 85.25:9.7:5:0.05 (mol%) for control LTSL (a Thermodox® like formulation [42]). Lipid stocks were combined in a round bottom flask in proportion to their respective mol% values (total mass of lipid 20-30 mg, as appropriate). The solvent was slowly evaporated *in vacuo* to ensure a thin and even

film formation. This was hydrated in 300 mM ammonium sulphate, pH 4.0 (1 mL) and XL750.DSA freeze/thaw (x 5) by alternately plunging into liquid nitrogen and then hot water to fragment the film. The resulting suspension was sonicated at 60 ^{o}C for just long enough to form a homogeneous, milky blue/white liquid. This was then extruded at least three times through a 100 nm polycarbonate membrane using a Northern Lipids (Burnaby, Canada) LIPEX extruder heated to 55 ^{o}C and pressurised to about 10-20 bar. The external buffer was exchanged to sterile 20 mM HEPES pH 7.4 with 5% glucose (w/v) using a PD10 size exclusion column (Amersham, Buckinghamshire, UK). The resulting, slightly cloudy, blue suspension was sized using a Nanoseries Nano ZS (Malvern Instruments, Worcestershire, UK) before incubation with topotecan hydrochloride (1 mg/mL aq.) at 38.0 °C for 1 h 20 (iTSL) or 37.0 °C for 2 h (LTSL). This drug-loading step was performed using a Thermocycler (Mastercycler Personal, Eppendorf, Stevenage, UK) in order to provide accurate temperature control. Excess, non-encapsulated drug was removed using a PD10 column loaded with HEPES buffer, giving a clear, yellow/green suspension. The size of the liposomes was recorded using a sample (100 µL) that was then employed to quantify the lipid and topotecan concentrations while the remainder was stored at 4 ^{o}C. Lipid concentrations were determined using a modified version of the Stewart assay. In brief, liposome samples (50 µL) were mixed with water (150 µL) and MeOH:$CHCl_3$, 1:1 (v/v) (200 µL) then vortex mixed with vigour giving an emulsion. The sample was centrifuged (4000 g; 2 min) to separate fully organic and aqueous layers. Thereafter, an aliquot (70 µL) of the organic layer was combined with Stewart reagent (5 µL, $FeCl_3$/NH_4SCN aq.), and the combination vortex mixed again then centrifuged. Finally, an aliquot (50 µL) was then transferred to a glass 96-well plate (Cayman Chemical, Ann Arbor MI, USA) and A_{455} value measured on a plate reader (Infinite 200 Pro, Tecan, Männedorf, Switzerland) for comparison with known standards. The topotecan concentration was measured by HPLC using the method described below. **Differential Scanning Calorimetry** was used to assess the iTSLs phase transition. iTSLs were diluted to ~ 1 mg/mL lipid into degassed 20 mM HEPES, 5 w% glucose buffer, pH 7.4. Samples (300 uL) were then loaded into a Nano DSC (TA Instruments,New Castle, DE, USA) and three rounds of sequential heating/cooling (25-70 ^{o}C at 1 ^{o}C/min) was then carried out against a reference of the same buffer. Each scan sequence was also carried out in triplicate with new samples of liposomes.

Topotecan release *in vitro*

Triggered drug release was assessed by fluorescence. Topotecan has a UV/visible absorbance profile that is pH-sensitive and undergoes a red shift from an A_{max} value of 385 nm at pH ~ 6.5 to a value of 414 nm at pH > 7.5. In a similar way topotecan solutions that are acidic are colourless, and those that are neutral/basic are coloured distinctly yellow. Since the central core of both the LTSLs and

iTSLs are acidic, fluorescence emission on excitation at the 414 nm band is greatly reduced for encapsulated topotecan. Once the drug is released into a neutral or basic solution, the shift in absorbance band is accompanied by a large increase in fluorescence. This is further enhanced by de-selfquenching effects on dilution (as seen with liposomal doxorubicin). Hence, by measuring changes in fluorescence intensity as a function of time upon incubation of liposome preparations at various temperatures, extent of drug release could be observed in real time. Studies were carried out with separate samples (50 µL) diluted 1:20 (v/v) in 20mM HEPES buffer then incubated in a Thermocycler (37-41 ^{o}C; 0-15 min) before being cooled to ambient temperature. After transfer to a 96-well plate, the absorbance (414 nm; b.w. 9 nm) and fluorescence (Ex 414 nm b.w. 9 nm; Em 530 nm b.w. 20 nm) emitted from individual samples were measured using a plate reader. Complete release was assessed after liposomes were sonicated (2 min; 60 ^{o}C) to allow topotecan to be released in the external buffer. Using the similar analytical method, iTSLs and LTSL both loaded with topotecan were incubated in 50:50 vol% of fetal bovin serum (FBS) to 20 mM HEPES pH 7.4 and drug leakage was monitored over time at 37 °C. iTSL containing topotecan were also tested for drug leakage over time in 20:80 vol% human plasma to 20 mM HEPES pH 7.4 at 35 and 37°C.

Pharmacokinetics and topotecan quantification by HPLC

All procedures on animals were conducted in accordance with UK Home Office regulation and the Guidance on the operation of the Animals (Scientific Procedures) Act 1986.

BALB/c mice were used for the majority of the pharmacokinetics studies. Mice were injected with topotecan iTSLs (8 mg/kg topotecan per mouse body weight) and drug pharmacokinetics were assessed by blood sample analyses. Blood samples (50-100 µL) were collected at time intervals (2 min – 4 h) and transferred into pre-weighed plastic vials containing heparin (5 uL). Plasma was isolated by centrifugation (3000 g; 4 min) and 50 µL were transferred to a 0.22 µm centrifuge tube filter (Spin-X; Nylon) with deionised water (450 µL). These tubes were centrifuged again and the filtrate transferred to covered HPLC vials. Batches of 5 samples were analysed three times using an HPLC. Samples were loaded in deionised water containing 0.1 % trifluroacetic acid and eluted with acetonitrile using the gradient: 0 min 0 %, 1.5 min 0 %, 5 min 50 %, 6 min 50 %, 7 min 0 %, 8.5 min 0 % and a flow rate of 3.5 mL/min. Detection was by absorbance (210 / 254 / 280 nm for proteins and other biologicals; 380 nm for topotecan; all using a bandwidth of 8 nm c.p. reference at 700 nm) and fluorescence (Ex 400 nm; Em 545 nm; PMT-gain 18). Topotecan could be reliably identified even at low concentrations (10-20 ng/mL) by its intrinsic fluorescence and retention time (3.33 ± 0.03 min; N = 45). Final blood concentrations of topotecan are given after correction for dilution effects during

sample preparation. To estimate the % injected dose (ID), the total plasma volume was defined as 1/26 (mL/g) of the body weight [43].

Cells inoculations in mice and tumor generation

IGROV-1 (ovarian cancer) cells were routinely cultured in RPMI-1640 medium supplemented with FBS 10 vol%. When cells reached 80-90 % confluence, they were prepared for implantation in mice. Cells were washed in saline and counted. Accordingly with the cell counting an equal volume of saline containing the cells was mixed with Matrigel (Gibco, Thermo Fisher Scientific, Waltham, MA USA). For tumour generations, $5x10^6$ cells contained in 50 % Matrigel were inoculated subcutaneously on both flanks of 8 week old SCID Hairless Outbred mice (SHO; Charles River, Germany). After 2 weeks, the formed tumours on each flank had reached an average diameter of 5-6 mm.

FUS positioning and induced hyperthermia in mice

Mice were prepared to receive FUS treatments using the Therapy and Imaging Probe System (TIPS; Philips, Netherlands). First, tissue temperatures were monitored by three fine-wire, T-type thermocouples implanted around the tumour. Thereafter, the mouse's flank was covered by degassed, warmed ultrasound gel and the TIPS transducer was placed at a distance of 88 mm from the target. This location was selected to place the FUS focal point slightly above the skin surface, reducing the risk of burns and achieving uniform heating throughout the tumor (as assessed by thermocouples). Each FUS treatment was delivered at the transducer natural frequency of 1.3 MHz, using a 99.9% cycle duty and 10-20 W of acoustic power depending on the local temperature variation required (following feedback from the thermocouples). Each FUS treatment was seen to raise the target tumour temperatures up to 42.0 ^{o}C that was then maintained for a further 3-5 min.

Nanoparticles biodistribution and drug release *in vivo*

The tumour bearing mice were injected intravenously with topotecan (8 mg/kg) iTSLs in an aliquot (200 µL) of sterile 20 mM HEPES pH 7.4 with 5 vol% glucose. The injections were performed with anaesthetised mice using a syringe driver holding the syringe connected to a cannula inserted in the tail vein of each mouse. The injection rate used was 400 µL/min. Immediately post injection, each anaesthetised animal was placed into the Maestro EX (Perkin Elmer, MA, USA) for NIRF imaging. The MaestroEX settings were adjusted to record topotecan (540 nm) or Xenolight (780 nm) fluorescence signal. Finally, the images were unmixed (multispectral analysis) using the Maestro 3.00 software, balanced using ImageJ [44]. Signal intensity or NIRF brightness from area matched regions (e.g.

centre of the tumour) of left and right tumours as well as shoulder point was quantified and plotted against time post-injection.

Magnetic Resonance Imaging

Anaesthesia was induced in mice using 5 % isoflurane-oxygen mix and maintained at 1.0 - 1.5 % isoflurane via a facemask throughout scanning. Mice were placed into a quadrature volume coil (39 mm inner diameter; RAPID Biomedical GmbH, Rimpar, Germany) and then into a 7 T horizontal bore VNMRS scanner (Agilent Inc., Walnut Creek, CA, USA) for MRI. T1-relaxometry was performed using a spin-echo sequence with the following parameters: repetition time (TR), 320, 800 and 2800 msec; echo time (TE), 12 msec; 2 averages; matrix size, 256 x 128; and field of view (FOV), 32 x 32 mm. Transverse contiguous slices (13, 2 mm thick), covering most of the xenografts on the flanks were collected. Temperature was maintained at 37 ^{o}C with warm air and respiration monitored throughout scanning (Small Animal Instruments, New York, USA).

T1 maps were calculated from the relaxometry data by pixel-by-pixel fitting to the equation: $SI = M_0 * 1\text{-}exp^{(-TR/T1)}$ using ImageJ where M_0 is the proton density and SI is the signal intensity at different values of TR. Areas of interest were placed on the T1 map to calculate T1 distribution histograms.

Results

iTSLs topotecan formulation and characterisation

iTSLs contained the MRI lipid Gd.DOTA.DSA (scheme 1) at 30 mol%. Nanoparticle physical properties varied slightly from batch to batch but representative values were as follows: i) average hydrodynamic diameter of 140 nm with a polydispersity index of 0.1-0.2, ii) final concentration of encapsulated topotecan 480 µg/mL (total lipid concentration 12 mg/mL) per batch. Differential Calorimetry analysis indicated a Tm of about 43 °C (supplementary information Figure S5)

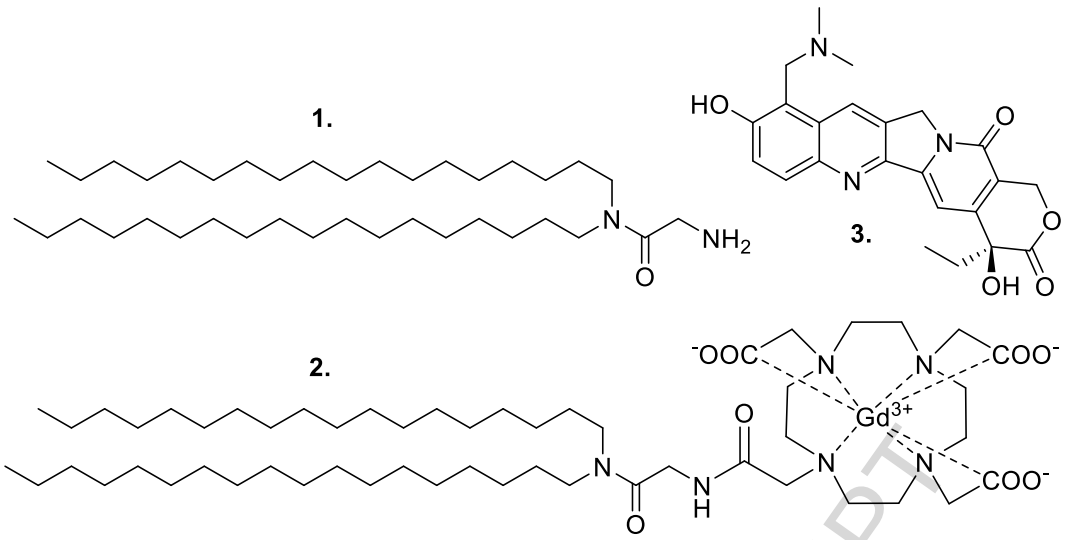

Scheme 1: Chemical structure diagrams for the parent **(1)** and MRI labelled lipid **(2)** and the encapsulated anticancer drug, topotecan **(3)** in the lactone state.

iTSLs Topotecan release was monitored by the changes in its intrinsic fluorescence (Ex 410 nm, Em 540 nm; Figure S1 Supplementary information); the combination of a shift in the pH-sensitive absorbance maximum and de-self-quenching resulted in a significant increased emission when topotecan was released from the low-pH aqueous core to neutral-pH buffer conditions (Figure 1). iTSLs were incubated in serum and plasma mixes with buffer and drug leakage was monitored for 30 min. Topotecan and NIR fluorescence were imaged pre- and post-thermally triggered drug release using the Maestro EX imager (Figure 1a). As expected, the Xenolight NIRF signal remains constant pre- and post- incubation at 42 °C indicating no temperature effect on its fluorescent emission, whereas topotecan fluorescence is low before release but clearly visible after the thermal treatment. Topotecan release as a function of temperature was assessed by monitoring changes in topotecan fluorescence over time on incubation in a thermocycler (Figure 1b). Fluorescence levels reached a plateau which is suggestive of complete release. Little change in fluorescence was observed over a 10 min at 37 ^{o}C consistent with stable encapsulation. By contrast, changes in fluorescence were consistent with complete release after incubation for 4 min at 41 ^{o}C. Using this data set, the thermal T_m of our liposomes was estimated as 40 ^{o}C (Figure 1b). TSLs have a characteristic tendency towards leaky lipid membranes in high serum buffers at 37.0 ^{o}C. The iTSLs show this with slow topotecan release ($t_{1/2}$ about 35 min) under these conditions (Figure 1c). When topotecan is encapsulated in LTSLs this leakage is more substantial compared to iTSL-topotecan (Figure S2 Supplementary information). Mechanistically, drug release is likely caused by pore formation resulting from thermally induced fluid mesophase transitions in lipid bilayers within which drug is encapsulated [45]. This characteristic has been observed previously when LTSL composition was investigated by Needham *et al*. [42]. It is likely that the presence of some bilayer soluble topotecan is responsible for this apparent leakage. Topotecan has three titratable functional groups

in a physiologically relevant pH range. A basic dimethylaminomethyl group in the A-ring (scheme 1) has a pK_a of approximately 10.5 whereas the phenolic hydroxyl group has a pK_a between 6.5 and 7.0. Weak solubility of topotecan in the bilayer would also account for the drug release in the *in vitro* assays for drug leakage [42].

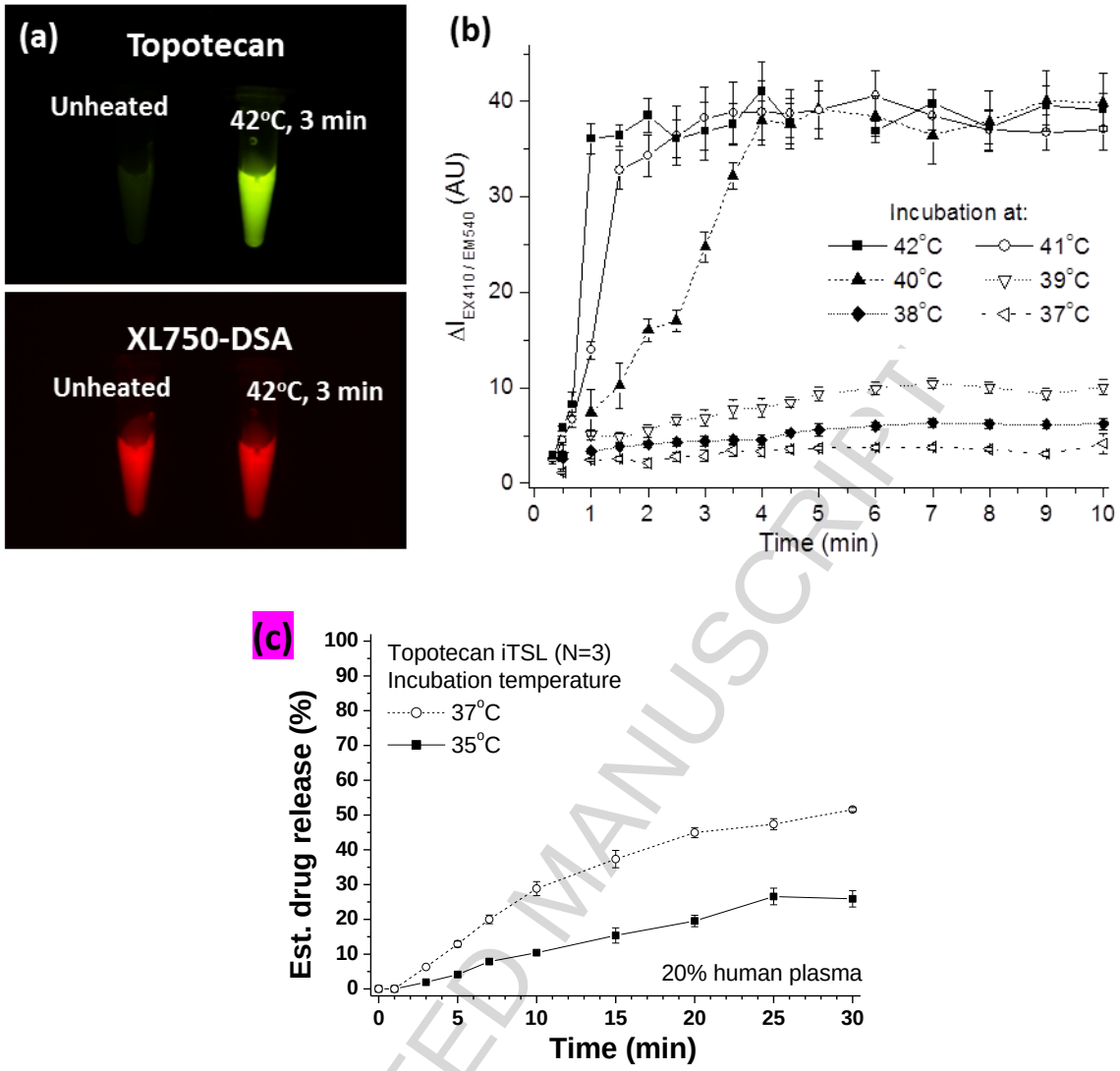

Figure 1: Topotecan release from thermosensitive liposomes monitored by intrinsic drug fluorescence (Ex 410 nm, Em 540 nm); **(a)** fluorescence imaging of unheated **(left)** and heated **(right)** liposomes shows an increase in topotecan emission in the visible spectrum **(top)** but no change in NIR from the XL750-labelled lipid; **(b)** topotecan release profiles in buffer after incubation at different temperatures indicate a critical T_m of 40 °C, error bars show n= 3+/- S.D.; **(c)** topotecan release from iTSL at 35.0 and 37.0 °C in 20/80 plasma/HEPES buffer.

In vivo pharmacokinetics of topotecan and clearance from blood

For the first *in vivo* study, control experiments were performed injecting topotecan iTSLs *i.v.* and monitoring their bio-distribution with the Maestro EX following the NIRF signal intensity over two weeks (Figure 2). Given the tissue depth sensitive nature of NIRF fluorochromes relative signal brightness was considered. At each time point of imaging, both dorsal and ventral images were collected to better assist assessing fluorescence biodistribution. In nearly all cases the NIRF

distribution was spatially and temporally conserved across animals (N = 3). At initial time points, the NIRF signal was found fairly even throughout body, consistent with vascular distribution (blood pool). Large near-surface blood vessels (e.g. in the hind legs) are visible for the first 30 min and larger tumour associated vessels may be located from 30-60 min. Subsequently, between 1 h and 4 h post injection the iTSL biodistribution began to narrow to bladder, liver/spleen (additional data Figure S4 upper panel No FUS) and the xenograft tumours (Figure 2a). After 24 h, nanoparticles' NIRF signal appeared to be mainly localised in the tumours and liver, with nothing apparent from the vasculature. After 2 weeks, NIRF signal was still observable allowing us to monitor iTSL lipid clearance from both liver and tumour target sites. These observations are broadly supported by the data of other researchers reported in their experiments using Cy5.5 labelled liposomes [46], indocyanine green (ICG) chemically modified liposomes [47] and PET/fluorescent labelled TSLs [48]. These results suggested an earlier peak tumour uptake than expected, between 6 h and 24 h. The spatio-temporal information regarding iTSLs biodistribution in tumours is critical as it can be used to timely applications of FUS.

In order to characterise the topotecan drug clearance, mice were injected (*i.v.* tail vein) with either topotecan liposomes or a concentration matched control of free topotecan in the same buffer. Fluorescence HPLC analysis of blood samples allowed the topotecan kinetics to be assessed as a function of time (Figure 2b), demonstrating that free drug is cleared from the blood circulation in minutes, while topotecan from liposomes was detectable in the blood pool for up to 2 h. Our conclusion that liposomal encapsulation prolongs topotecan half-life in plasma is broadly supported by the results of other researchers, using topotecan encapsulated in conventional liposomes [49]. Comparing the pharmacokinetics of thermosensitive against non-thermosensitive liposomal topotecan formulations indicates that the former have a substantially shorter half life (as would be expected). Knowledge of the iTSL-drug plasma pharmacokinetics can be used to optimise hyperthermia protocols by selecting the timings for hyperthermia application. A finely tuned pharmacokinetic profile of thermosensitive liposomes in combination with FUS application could significantly improve the therapeutic profile.

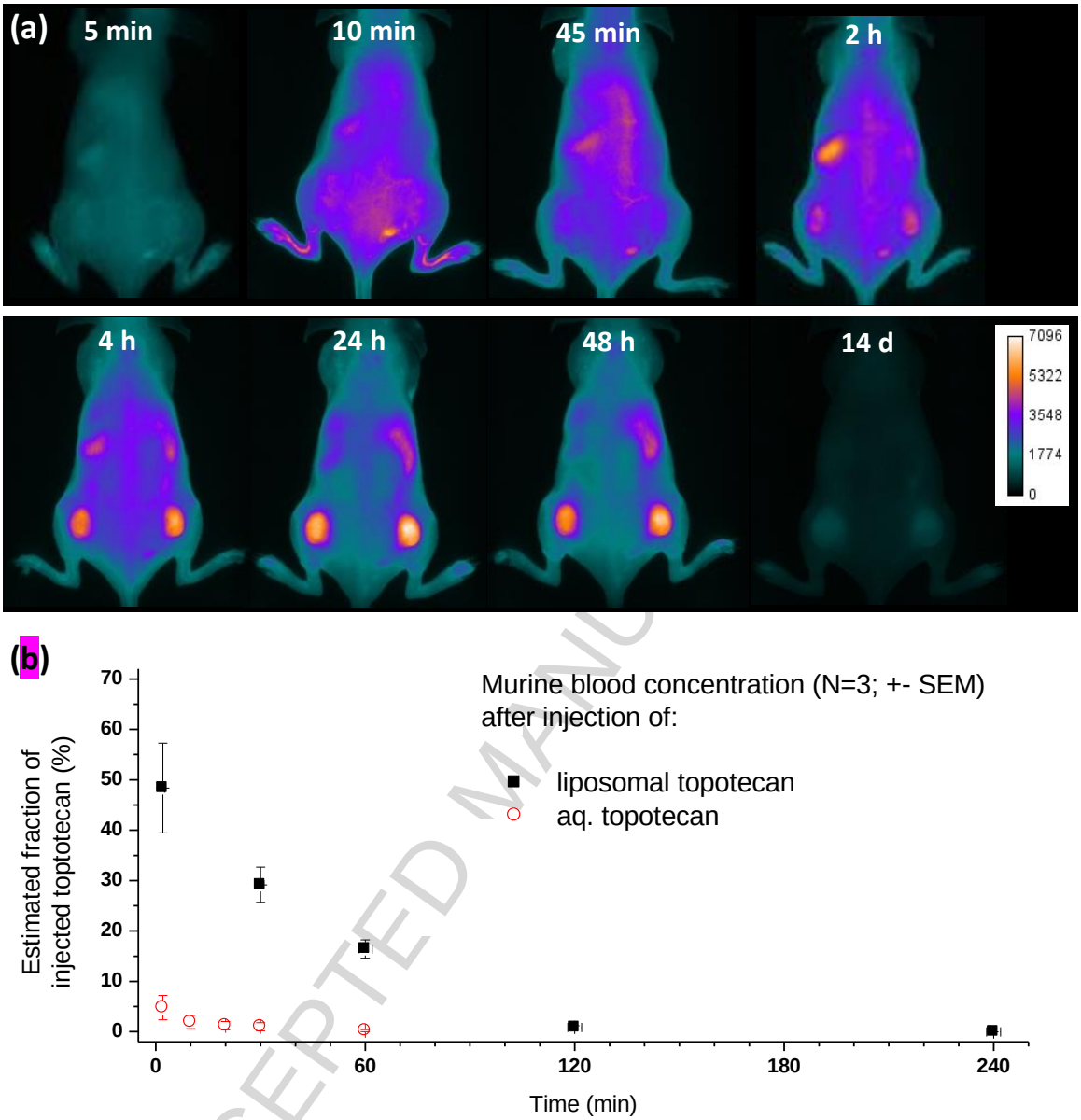

Figure 2: *In vivo* distribution of iTSLs topotecan in the absence of FUS hypothermia; **(a)** NIRF tracking the XL750-labelled lipid post injection (200 µL; tail *i.v.*) of topotecan liposomes to a xenografted mouse with tumours on each haunch. Imaging was under anaesthetic using a Maestro EX multispectral analyser, with fluorescence excitation at 704 nm and emission collected in 10 nm steps over 740 – 950 nm. After spectral un-mixing of the XL750 signal (c.p. liposomes in buffer) the images were contrast adjusted and false coloured using ImageJ [44]; **(b)** HPLC quantification of blood bourn topotecan. Groups of mice (N = 3) were injected (*i.v.* tail) with either liposomal topotecan or a matched concentration of free drug in the same buffer. Small (~ 50 µL) blood samples were then collected over 4 h, before analysis by reverse phase HPLC with UV/vis and fluorescence detection.

Therapy imaging probe system (TIPS) and short FUS treatments

The liposome pharmacokinetics showed a clear accumulation in the tumours and liver 4 h post *i.v.* injection (Figure 2 and Figure S4), while free unencapsulated topotecan had a very brief blood half-

life (few minutes only; Figure 2b). In order to improve this intrinsic biodistribution and favour tumour uptake we applied FUS on the right side using the preclinical TIPS transducer..

The effect of the FUS treatment on the pharmacokinetic behaviour was then monitored with the NIRF-imager, and the control of the temperature induced by FUS was achieved by placing two thermocouples (TC1 and TC2) around the target tumour. Manual control of the applied power allows the tumour temperature to be constrained by < 1^{o}C for a treatment period of 3-5 min. Our target was 42 ^{o}C to the top thermocouple and 39 ^{o}C for the bottom, indicating an internal temperature of about 40-41 ^{o}C (Figure S2 Supplementary information). Given the small size of the tumours (around 5 mm diameter) and their location just below the skin we decided to use far-field FUS temperature conditions. This places the focal point about 6-8 mm away from the skin surface ("off focus") and avoids the risk of burns (particularly around the thermocouples or due to unintended entrapped air bubbles between skin and gel).

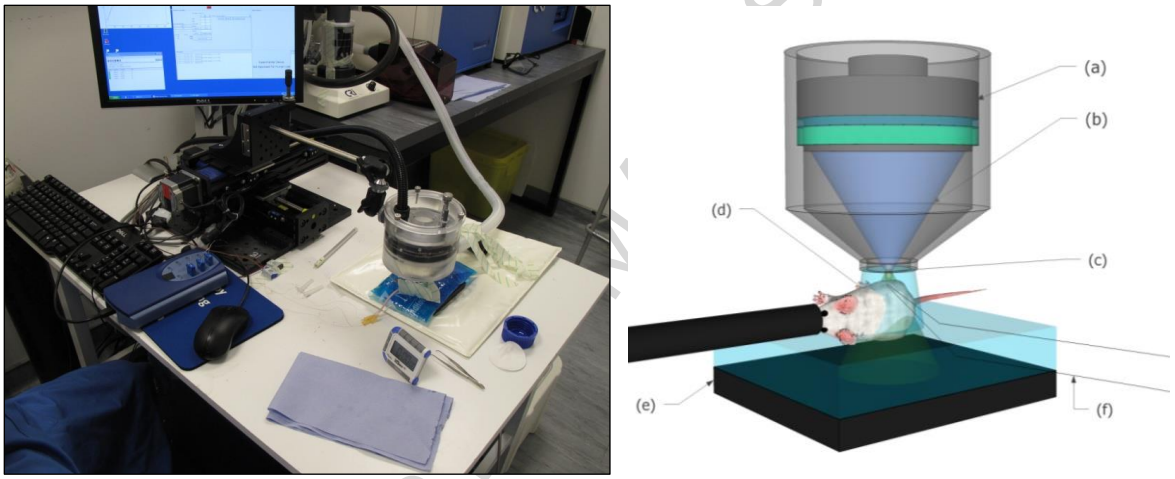

Figure 3: TIPS focused ultrasound (FUS); **(left)** overview of the equipment showing the water-filled transducer chamber, the thermocouple interface, and the control PC; **(right)** schematic of the in vivo configuration with the transducer **(a)** raised such that the ultrasound biconic **(b)** focuses just above the skin surface over the tumour **(c)**. The mouse is surrounded with warmed, degassed ultrasound gel **(d)** and placed on an ultrasound absorbing mat **(e)** to prevent reflections off the table. Temperature monitoring is via two or three fine-wire thermocouples **(f)** implanted around the tumour.

FUS protocols using NIRF imaging for guidance

According to this protocol (Figure 4a), a brief, mild FUS treatment was applied (5 min, ≤ 42 ^{o}C) to the right xenograft tumour, 30 min post *i.v.*-administration of topotecan iTSLs (the other tumour

representing a non-FUS control). We observed a very significant increase in NIRF signal intensity in the FUS treated tumour just 10 min after FUS application (time point 40 min in Figure 4b). This signal continued to increase at least during the next 3 h and resulted in a permanent enhancement of NIRF on the right tumour of the animal for the 3 week period of the experiment (see Figure 4b). Four of the animals were sacrificed after a week and both tumours were excised and imaged with clear difference between the FUS-treated and non-treated sides. This suggests that the single FUS treatment was sufficient to enhance substantial and selectively partition of iTSLs blood pool into FUS treated tumours. Moreover, the tissue persistence of the NIRF signal *in vivo* post FUS treatment was found to extend out to at least 3 weeks, albeit with significant loss of intensity over time (possibly due to destruction of the fluorophore, clearance from the tumour site, and/or due to tumour cell death). This offers the possibility of following the effects of the treatment by simple NIR signal observation post intervention.

In parallel, changes in topotecan intrinsic fluorescence (Ex 435-480 nm, Em 500-720 nm in 10 nm steps) was monitored in order to determine time and location of the released drug from liposomes. Since released topotecan has a short half-life *in vivo,* the fluorescence observed after FUS treatment is rather transient. Despite this, the large fluorescence increase after FUS treatment of tumours indicates the drug release from the liposome core (see Figure 4c). The topotecan related fluorescence signal did not persist in the tumour beyond 1 h post-FUS likely as a result of either drug elimination, drug metabolism or DNA target site intercalation in the topoisomerase-I cleavage complex (topotecan is a topoisomerase I inhibitor) [49]. Topotecan undergoes reversible, pH-sensitive ring-opening hydrolysis [50].

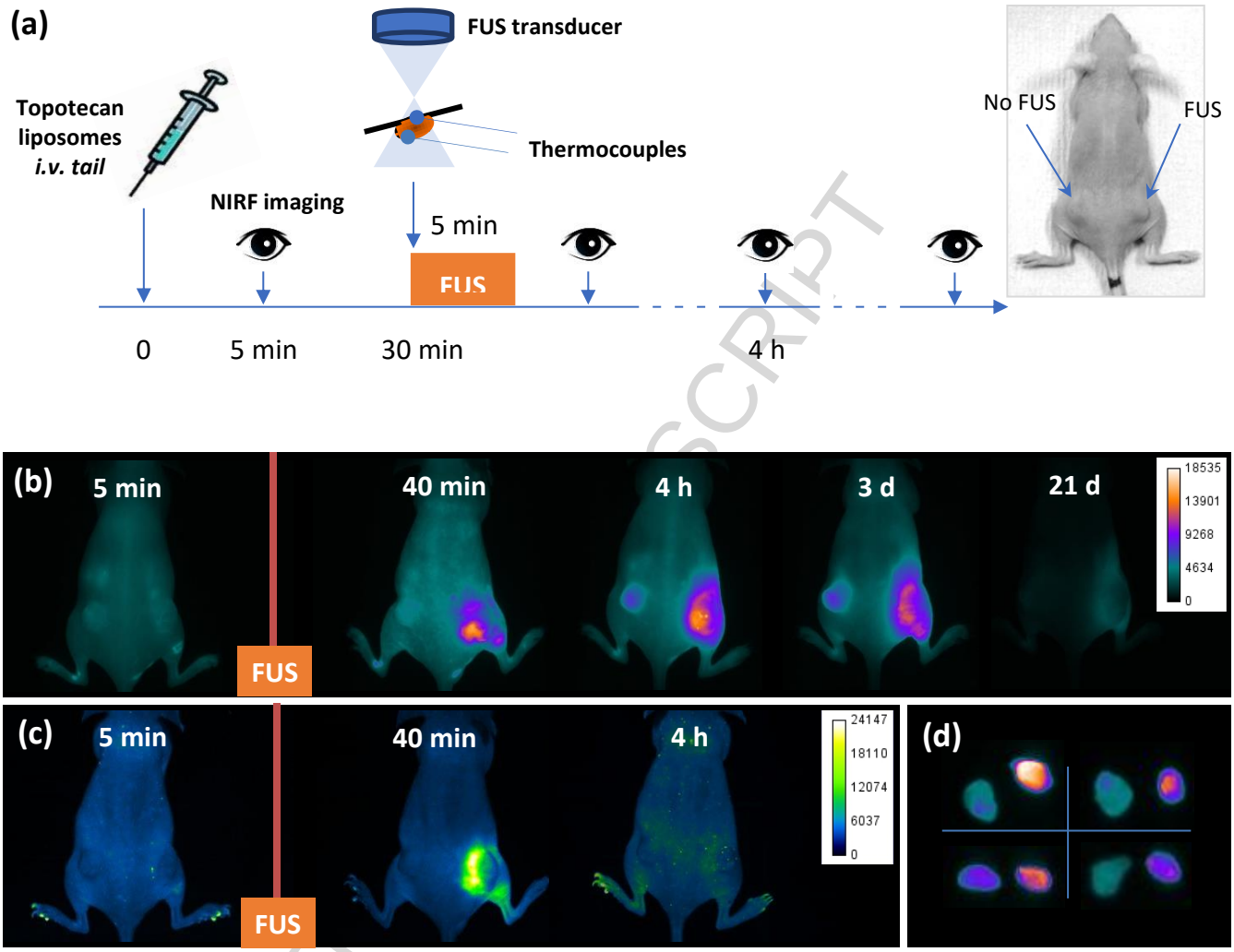

Figure 4: Changes in liposome distribution due to FUS hypothermia (5 min; ≤ 42 °C) to the tumour on the right haunch, 30 min post injection (200 µL; tail *i.v.*); **(a)** Procedure schematic showing timings of the injection, FUS treatment and fluorescence imaging at intervals up to 21 days. Imaging was carried out as previously described for **(b)** XL750-labelled lipid and **(c)** topotecan intrinsic fluorescence. FUS-induced release of topotecan can be seen as suddenly increased 550 nm emission immediately after treatment. This signal is transient and lost by the 4 h point. The bright signal seen on the animal's feet is an artefact and due to autofluorescence from the claws. Full body XL750/topotecan images are from one mouse followed for 3 weeks, four others were sacrificed after 1 week and **(d)** the tumours excised and imaged for XL750 fluorescence.

To promote even more drug delivery in the treated tumour, a repetition of the FUS protocol was developed (Figure 5a) wherein the two treatments were applied within the 2 h window estimated from the liposomal topotecan blood clearance result. Previous studies have shown a 1-2 h lag time for onset of the liposomal drug distribution in tumour [16] [51]. Therefore, we used information from both the pharmacokinetics data and tumour biodistribution from imaging to identify the optimum timing of the hyperthermia treatments. In this protocol we suggest the application of FUS treatment post administration and simultaneous with the time liposomes start reaching the tumour through blood it can lead to higher liposome extravasation and distribution in tumour. FUS was applied at 30 min post *i.v.* injection (for 3 min; ≤ 42 ^{o}C) and at 90 min post i.v. injection (5 min; ≤ 42 ^{o}C) at the right tumour as before. Imaging for NIRF and topotecan intrinsic fluorescence was carried out before and after each FUS treatment and then as described above. Prior to the second FUS, a substantial accumulation iTSLs as seen by the increase of the NIRF signal was already observed in the treated tumour, this signal build up was further incremented following the application of the second hyperthermia (Figure 5b). The sequential repetition of FUS treatment induced an accentuated enhanced permeability effect ([52] and Figure S3 and S4) , showing a clear correlation between thermal dosing (repetition of heating) and hyper-permeability of the vasculature of the targeted tumour.

In Figure 5b, when changes in topotecan-related fluorescence were monitored, substantial fluorescence signal was observed after both the first and second FUS pulses, consistent with substantial FUS-induced drug release following both treatments. In conclusion, repeated FUS treatments show that increasing the temperature will increase iTSL accumulation in the heated area in a synergistic way. In addition a burst release of topotecan will be obtained after each FUS application if it is applied during the plasma kinetics window.

Figure 6 represents the results of the signal intensity analysis and estimation of signal intensity of tumours' ROI as well as signal coming from non tumour tissue. The area under the curve signal intensity versus time was estimated and plotted. It is clear that animals receiving focused ultrasound treatments on their right tumour presented an increase in signal brightness consistent in all animals. The animals that received twice the treatment showed an even brighter tumour area. Left tumours showed low signal intensity independent the number of FUS treatments the right tumour had and control areas like shoulder muscle showed the same intensity consistently.

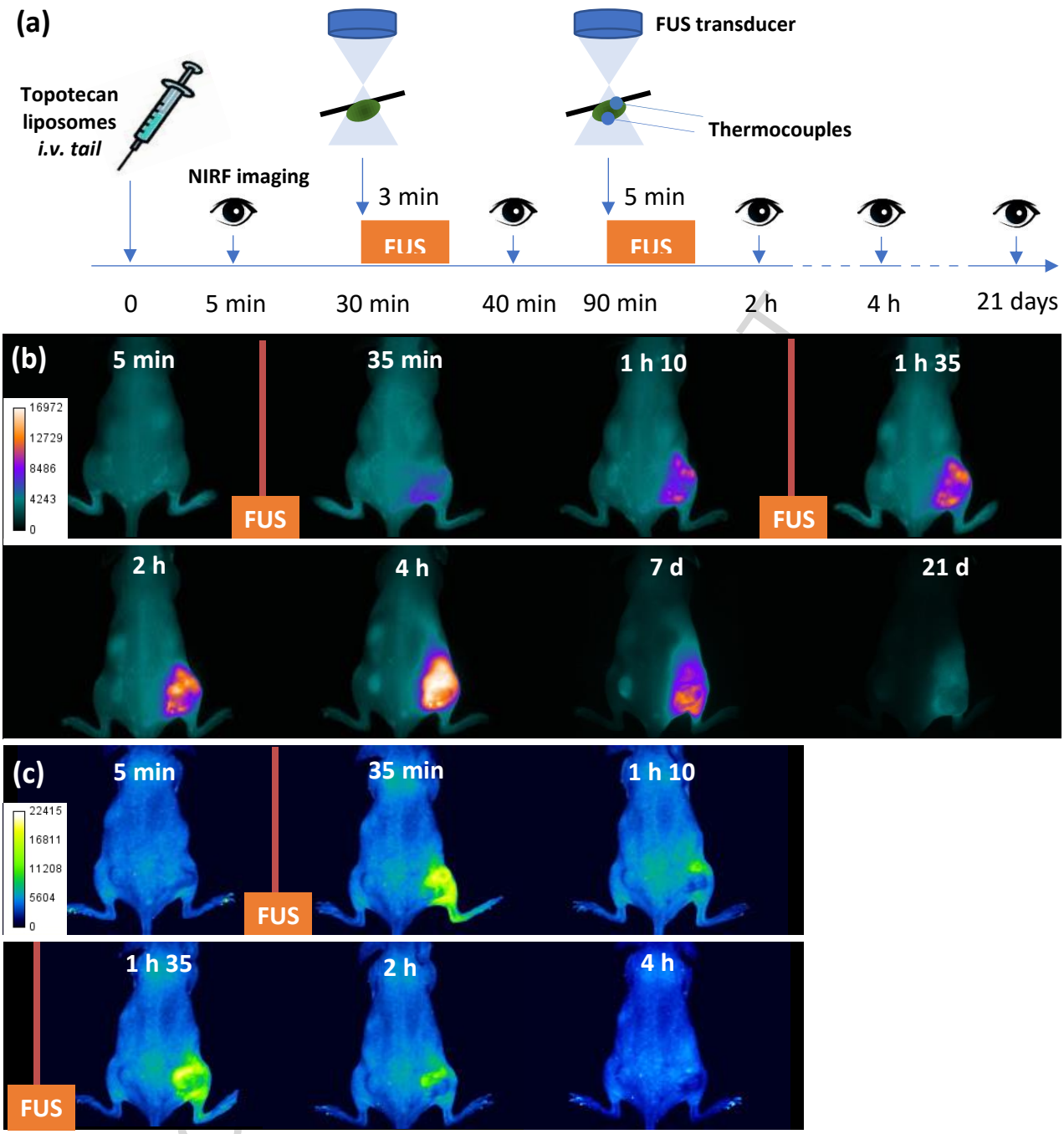

Figure 5: Two FUS applications significantly increases liposome uptake; (a) Schematic of a double FUS application to the right-hand tumour. This combines an initial treatment (3 min; ≤ 42 °C) at 30 min with a slightly longer one (5 min; ≤ 42 °C) one hour after. As before, image stacks are collected at time points up to 21 days. **(b)** XL750 imaging shows increased liposome uptake after treatment. **(c)** Intrinsic topotecan fluorescence in also seen to transiently increase after each FUS. Results are from a single representative mouse (N = 3).

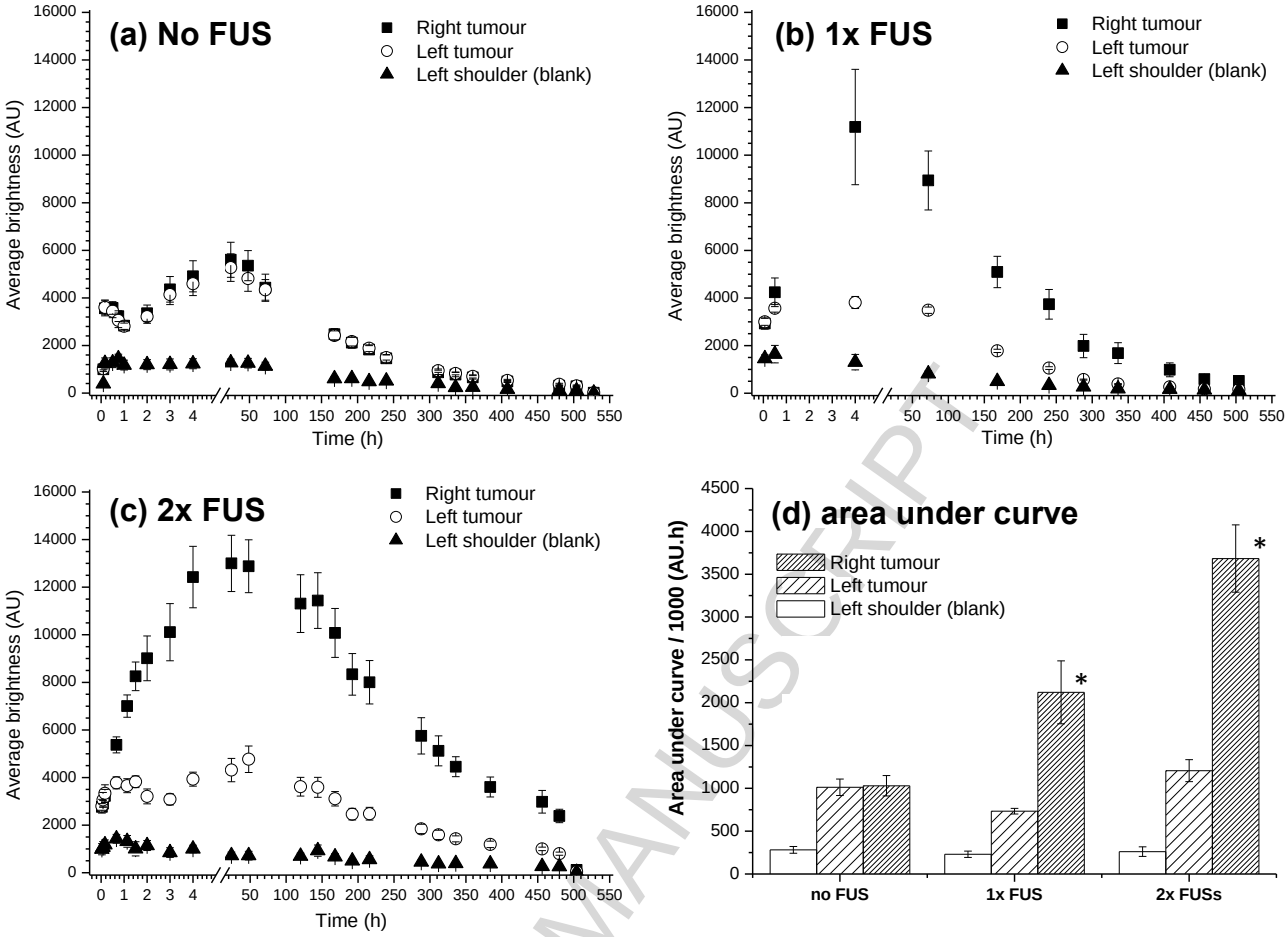

Figure 6: NIRF signal intensity presented as average brightness calculated from ROI (regions of interest); (a) NIRF signal intensity coming from tumours compared to signal coming from shoulder; no FUS treatment; **(b)** NIRF signal intensity coming from left (untreated) and right (1x FUS treated) tumour; **(c)** NIRF signal intensity coming from left (untreated) and right (2x FUS treated) tumour; **(d) Estimated areas under the curve** of untreated and the FUS treated tumours. * corresponds to statistical difference $p < 0.05$ t–test.

MRI imaging confirms the enhanced accumulation of the iTSLs in tumours as seen by NIRF imaging

The iTSL formulation we have developed and presented here has the advantage of being labelled with Gd.DOTA.DSA and XL750.DSA. The inclusion of an MRI sensitive lipid incorporated in the lipid bilayer makes this formulation applicable to be used with MRI guided FUS (MRgFUS) as used in the clinic. The aim here is to test the hypothesis that this formulation's tumour accumulation can be imaged by MRI and corresponds to NIRF observations. We used the ability of Gd.DOTA.DSA liposomes to decrease T_1 and enhance contrast as a method to confirm the distribution of the liposomes in the tumours after the FUS treatments. Mice were treated with FUS and imaged using

NIRF before being set to be imaged by the 7 T MRI scanner. At 5 h post injection and after two FUS treatments MRI showed an enhanced decrease in the T_1 of the right tumour compared to the left tumour indicating the effect of the Gd.DOTA tumour labelling after the FUS treatment. It is likely that increased iTSLs accumulation in the hyperthermia treated tumour increased the Gd.DOTA.DSA lipid that leads to T_1 decrease. This experiment confirmed the results seen using optical imaging (Figure 7).

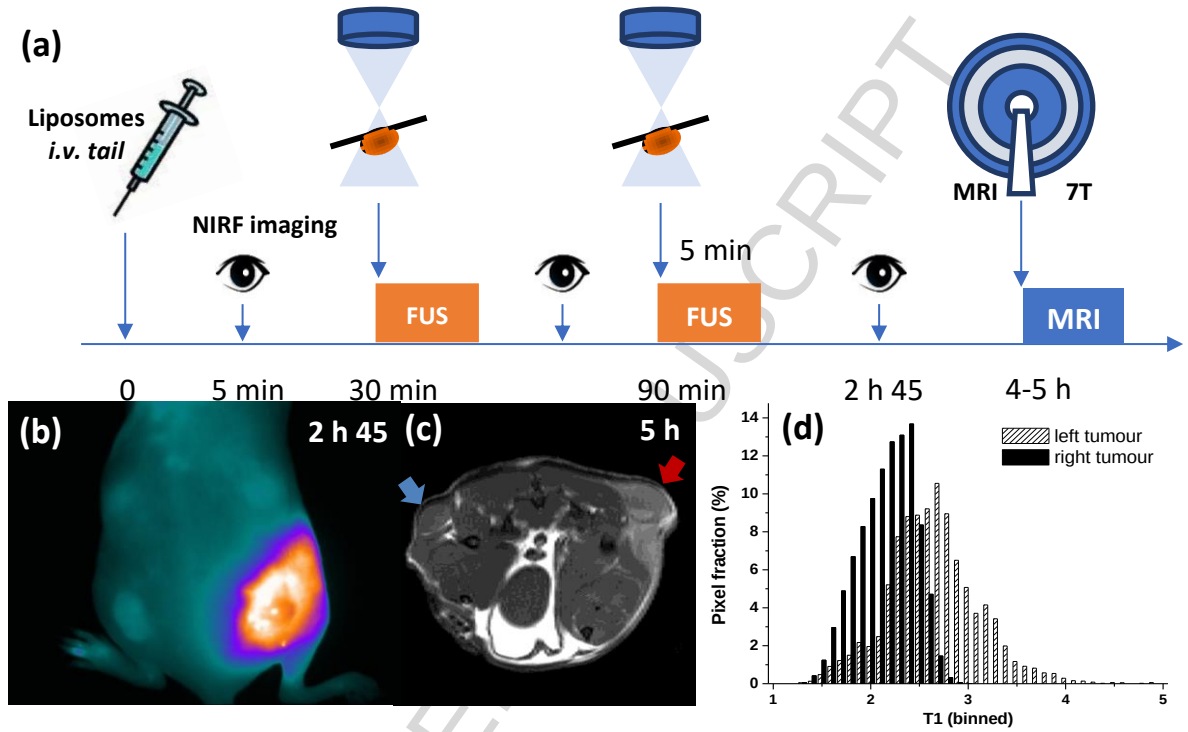

Figure 7: MRI imaging after dual FUS application; (a) Schematic showing FUS applications to the right-hand tumour followed by fluorescence and MRI imaging; **(b)** iTSLs imaging by optical and **(c)** T_1-weighted MRI imaging (field 7 T, TR 320 ms). The same mouse was injected *i.v.* with empty iTSL (without topotecan to avoid the risk of toxicity-induced MRI changes) and was treated twice by FUS treatment applied to the right tumour at 30 min and 1 h 30 min. NIRF imaging shows the treated mouse in dorsal view at 2 h 45 post injection. Two hours later on the same animal an MRI scan was performed. One axial slice is shown cutting through the region of the flank tumours, these are marked with blue (no FUS) or red (FUS) arrows; **(d)** the left and right tumours T_1 relaxation histograms.

Discussion

The development of image guided drug delivery using nanosized iTSLs is a potentially powerful technology for personalized medicine [53]. There is also a growing interest in the use of imaging tools to study nanoparticle biodistribution over time, and non-invasive triggers to promote controlled, localised drug release (theranostics nanoparticles) [39, 53]. PEGylated liposomes are proving to be increasingly popular vehicle for drug delivery [54]. The development of TSLs, such as Thermodox® is part of a trend of developing liposomes into more sophisticated platforms [55]. Others describe TSLs with encapsulated MRI contrast enhancement agents such as manganese or [Gd(HPDO$_3$A)(H$_2$O)] to monitor drug release in the tumour after application of HIFU [56, 57]. The work described here draws from this background and from our previous studies with gadolinium (III) (Gd)-bearing, imaging liposomes intended to act as positive contrast agents for the MRI of cancerous lesions *in vivo* [34-37]. Here, we have described the development of a thermo-responsive liposome with both MRI and NIRF imaging labels. These demonstrate physical properties that appear to synergise with brief FUS-induced mild hypothermia leading to enhanced partition of nanoparticles from blood pool to FUS-treated tumours, combined with controlled release of the encapsulated therapeutic cargo.

Hyperthermia has shown synergistic effects with neo-adjuvant chemotherapy and radiotherapy in clinic, improving existing treatments [9]. As a clear demonstration of the importance of mild hyperthermia, Li *et al.* [58] have shown significant effects from water bath heating on anti-tumour effects of their formulations. Since every tumour is believed to have a significantly different interstitial fluid flow and/or matrix density, a big challenge remains in the vascular permeation of the tumour in order to improve the drug delivery. Local hyperthermia appears to increase the pore sizes in tumour vasculature, decrease hydrodynamic hindrances, such as the ones induced by the intratumoral interstitial fluid flow and pressure in a manner that might facilitate nanoparticle (~ 100-150 nm in diameter) extravasation. Hyperthermia may also increase local blood perfusion in order to modify the pharmacokinetics of any particulate delivery system in the heated volume [59]. Such potential hyperthermia effects in tumours were reported by Kong *et al.* [60]. Mild hyperthermia (41 ^{o}C for 1 h) has also been reported to generate gaps in the endothelial lining of up to 10 µm [58], for at least 8 h. This supported similar observations by Kong *et al.* in a previous study [61]. However, we cannot rule out that other more FUS selective mechanisms (such as cavitation) are also involved given the magnitudes of the effects and synergies that we have observed and described above. In addition, our use of image guidance may assist in overcoming one perceived weakness of FUS treatment, namely drug wash out from the FUS treated tumour exacerbated by premature release

taking place prior to arrival of nanoparticle carrier in the tumour [53]. Recent studies presented by Koning *et al.* also indicated the effect of repetition of hyperthermia treatment on nanoparticle tumour distribution. In their study the two hyperthermia treatments are long (1 hour) induced by waterbath and no image guidance is given [62]. In a recent study prepared by the Koning team (corresponded by H. Grüll) liposomes labelled with 0.1% DSPE.DTPA In^{111} label for SPECT/CT were administered through a two stage heating protocol one before injection and one 4 h post injection showing that the two stage HT treatment protocol has substantial advantages [63]. In our study presented here we apply the repeated FUS protocols sequentially post injection. The rational for this protocol is to investigate treatments that could be translated to the clinic and apply imaging of the liposomes and FUS treatment in the MRI labelled lesions. Similar approach has been suggested by Tagami et al. [29]. Two different approaches on the method of hyperthermia treatments in combination with TSLs have been noted in literature. One that applies hyperthermia before injection and the second approach that applies hyperthermia post-injection. In the study we present here we investigate the hypothesis that the iTSLs will function first as diagnostic agents (labelling tumours) that will guide the application of focused ultrasound. We also use a non-long circulating liposome to avoid exposure of the healthy tissues to the cytotoxic for several hours. However, these liposomes circulate for a suitable time to allow FUS treatments. In our case we propose the use of imaging to guide the application of FUS for short (5 min) and repeatable hyperthermia treatments. Such short treatments have potentially the advantage of better compliance and translation to the clinic. Short hyperthermia treatments also have the advantage of being repeated several times during the plasma circulation time allowing for maximum tumour drug accumulation.

In this study we prepared a lipid that attributes the property of MRI contrast enhancement. Others have used contrast enhancing agents encapsulated within the core [57, 64, 65]. In our study we prepared a lipid coupled to DOTA.Gd to be part of the lipid membrane as this type of liposomes have shown improved T_1 decrease values due to their headgroup availability to interact with water [66]. It has been previously reported that Gadolinium based contrast enhancement agents can interfere with proton resonance frequency shift (PRFS) magnetic resonance (MR) thermometry indicating a 2° C change [67] . It was suggested in that study that shorter FUS treatment (similar to the ones used here) could overcome the effect of this change [67].

In our present studies, only mild hyperthermia protocols were used, 42 ^{o}C was selected as the temperature considered as safe (does not cause tissue ablation over this short time frame). Timings and the lengths of the hyperthermia were selected based on preliminary studies based on the blood clearance of the drug and the modulation of the iTSLs' biodistribution observed by NIRF

imaging. Optical imaging proved to offer a simple and cost efficient way to study biodistribution in the tumour. One of our clear observations was a synergism between short and moderate intensity FUS applications and iTSLs uptake. As a direct consequence, topotecan release was obtained in the tumour simultaneously to enhanced liposome uptake. After the first FUS, the liposomes' accumulation as well as the triggered drug release did not appear to be saturated events. Thus, the repetition of FUS treatments amplified the phenomenon of uptake ascribed to an increase of "hyperpermeability" of the treated tumour. This drug release can become an on-demand process, based on the therapeutic window offered by the formulation and the FUS protocol used.

Different hyperthermia-dependent drug release mechanisms have been termed as intravascular and interstitial release [5]. In our double FUS experiment, the first release would be mainly an intravascular release and the second release would be a mixture of interstitial release for the TSLs already accumulated in the tumoral tissue and intravascular for the nanoparticles still circulating in the blood stream. Studies using larger animals, proper labelling of carriers, and clinical equipment (e.g. MRgFUS) will provide better information on the effect of FUS treatment protocols.

The choice of topotecan in our studies was for reasons of drug-related fluorescence detection *in vivo so* we can monitor both drug and iTSLs using the same platform. This drug binds to topoisomerase I-DNA complex and prevents re-ligation of single strand breaks. Since it is FDA approved, this makes it a valuable tool in many treatment regimens. Nevertheless, as we observed in the blood clearance, the free drug is rapidly lost from body so ensuring encapsulation in liposomes is imperative [68]. However any number of other anti-cancer agents or combinations could also be encapsulated this way. Of these, doxorubicin and/or cis-platin are particularly favoured as potent anti-cancer agents with a reasonably generic use profile. iTSLs combined with FUS may find better use for the delivery of potent but highly toxic anticancer agents.

In recent studies using doxorubicin TSLs, FUS ablation was suggested as a new strategy to be combined with drug delivery systems (thermosensitive or not) [31, 69]. Both presented studies show an impressive efficacy of this method of FUS treatments (ablation / hyperthermia) in combination with thermosensitive liposomes. There is a need to investigate various protocols and combinations of focused ultrasound induced heating (hyperthermia and or ablation) with different drug therapies. It is also becoming clear that predictive math modelling of heat and drug diffusion in tissues and tumours should be sought to design and optimise image guided FUS triggered drug therapies.

Conclusion

In this study we have formulated a theranostic novel dual MRI/NIRF labeled nanoparticle (iTSL) that encapsulated the anti-cancer agent topotecan and enables real time imaging, making use of pre-clinically and clinically relevant imaging modalities. Image-guidance in turn enables the application of brief, moderate intensity FUS treatments that greatly increase iTSL uptake, and induce on-demand drug release mainly within the tumour volume. Should these effects be translated to the clinic, this suggests substantial benefits to cancer patients and improvements of the standard of the chemotherapy treatments for both primary and metastatic tumours.

Acknowledgements

The authors would like to acknowledge EPSRC (EP/I001700/1) and King's Commercialisation Institute (King's College London) for the financial support of this project. The support and advice on regulatory issues by EuNCL (European Nanotechnology Characterisation Laboratory) is acknowledged. M. Amrahli acknowledges scholarship support by the Ministry of Education of Republic of Azerbaijan. We need to acknowledge Dr Gerben Koning (deceased Dec 2015) for the inspiration and his vision legacy in the topic of hyperthermia.

References

[1] A. Babu, A.K. Templeton, A. Munshi, R. Ramesh, Nanodrug delivery systems: a promising technology for detection, diagnosis, and treatment of cancer, AAPS PharmSciTech, 15 (2014) 709-721.
[2] A.C. O'Farrell, S.D. Shnyder, G. Marston, P.L. Coletta, J.H. Gill, Non-invasive molecular imaging for preclinical cancer therapeutic development, Br J Pharmacol, 169 (2013) 719-735.
[3] E.G. Troost, D. Thorwarth, W.J. Oyen, Imaging-Based Treatment Adaptation in Radiation Oncology, J Nucl Med, 56 (2015) 1922-1929.
[4] S. Qin, B.Z. Fite, M.K. Gagnon, J.W. Seo, F.R. Curry, F. Thorsen, K.W. Ferrara, A physiological perspective on the use of imaging to assess the in vivo delivery of therapeutics, Ann Biomed Eng, 42 (2014) 280-298.
[5] Z.S. Al-Ahmady, C.L. Scudamore, K. Kostarelos, Triggered doxorubicin release in solid tumors from thermosensitive liposome-peptide hybrids: Critical parameters and therapeutic efficacy, Int J Cancer, 137 (2015) 731-743.
[6] S. Brown, D.R. Khan, The treatment of breast cancer using liposome technology, J Drug Deliv, 2012 (2012) 212965.
[7] J. Lao, J. Madani, T. Puertolas, M. Alvarez, A. Hernandez, R. Pazo-Cid, A. Artal, A. Anton Torres, Liposomal Doxorubicin in the treatment of breast cancer patients: a review, J Drug Deliv, 2013 (2013) 456409.
[8] M.R. Horsman, Tissue physiology and the response to heat, Int J Hyperthermia, 22 (2006) 197-203.
[9] J.P. May, S.D. Li, Hyperthermia-induced drug targeting, Expert Opin Drug Deliv, 10 (2013) 511-527.
[10] W. Rao, Z.S. Deng, J. Liu, A review of hyperthermia combined with radiotherapy/chemotherapy on malignant tumors, Crit Rev Biomed Eng, 38 (2010) 101-116.
[11] Y. Dou, K. Hynynen, C. Allen, To heat or not to heat: Challenges with clinical translation of thermosensitive liposomes, J Control Release, 249 (2017) 63-73.
[12] S. Dromi, V. Frenkel, A. Luk, B. Traughber, M. Angstadt, M. Bur, J. Poff, J. Xie, S.K. Libutti, K.C. Li, B.J. Wood, Pulsed-high intensity focused ultrasound and low temperature-sensitive liposomes for enhanced targeted drug delivery and antitumor effect, Clin Cancer Res, 13 (2007) 2722-2727.
[13] J.N. Weinstein, R.L. Magin, M.B. Yatvin, D.S. Zaharko, Liposomes and local hyperthermia: selective delivery of methotrexate to heated tumors, Science, 204 (1979) 188-191.
[14] M.B. Yatvin, J.N. Weinstein, W.H. Dennis, R. Blumenthal, Design of liposomes for enhanced local release of drugs by hyperthermia, Science, 202 (1978) 1290-1293.
[15] G.R. Anyarambhatla, D. Needham, Enhancement of the phase transition permeability of DPPC liposomes by incorporation of MPPC: A new temperature-sensitive liposome for use with mild hyperthermia, J Liposome Res, 9 (1999) 491-506.
[16] M.L. Hauck, S.M. LaRue, W.P. Petros, J.M. Poulson, D. Yu, I. Spasojevic, A.F. Pruitt, A. Klein, B. Case, D.E. Thrall, D. Needham, M.W. Dewhirst, Phase I trial of doxorubicin-containing low temperature sensitive liposomes in spontaneous canine tumors, Clin Cancer Res, 12 (2006) 4004-4010.
[17] D. Needham, M.W. Dewhirst, The development and testing of a new temperature-sensitive drug delivery system for the treatment of solid tumors, Adv Drug Deliv Rev, 53 (2001) 285-305.
[18] B.J. Wood, R.T. Poon, J.K. Locklin, M.R. Dreher, K.K. Ng, M. Eugeni, G. Seidel, S. Dromi, Z. Neeman, M. Kolf, C.D. Black, R. Prabhakar, S.K. Libutti, Phase I study of heat-deployed liposomal doxorubicin during radiofrequency ablation for hepatic malignancies, J Vasc Interv Radiol, 23 (2012) 248-255 e247.
[19] R.T. Poon, N. Borys, Lyso-thermosensitive liposomal doxorubicin: an adjuvant to increase the cure rate of radiofrequency ablation in liver cancer, Future Oncol, 7 (2011) 937-945.

[20] W.Y. Tak, S.M. Lin, Y. Wang, J. Zheng, A. Vecchione, S.Y. Park, M.H. Chen, S. Wong, R. Xu, C.Y. Peng, Y.Y. Chiou, G.T. Huang, J. Cai, B.J.J. Abdullah, J.S. Lee, J.Y. Lee, J.Y. Choi, J. Gopez-Cervantes, M. Sherman, R.S. Finn, M. Omata, M. O'Neal, L. Makris, N. Borys, R. Poon, R. Lencioni, Phase III HEAT Study Adding Lyso-Thermosensitive Liposomal Doxorubicin to Radiofrequency Ablation in Patients with Unresectable Hepatocellular Carcinoma Lesions, Clin Cancer Res, (2017).
[21] J. Tu, J. Ha Hwang, T. Chen, T. Fan, X. Guo, L.A. Crum, D. Zhang, Controllable in vivo hyperthermia effect induced by pulsed high intensity focused ultrasound with low duty cycles, Appl Phys Lett, 101 (2012) 124102.
[22] A.H. Negussie, P.S. Yarmolenko, A. Partanen, A. Ranjan, G. Jacobs, D. Woods, H. Bryant, D. Thomasson, M.W. Dewhirst, B.J. Wood, M.R. Dreher, Formulation and characterisation of magnetic resonance imageable thermally sensitive liposomes for use with magnetic resonance-guided high intensity focused ultrasound, Int J Hyperthermia, 27 (2011) 140-155.
[23] M. de Smet, S. Langereis, S. van den Bosch, H. Grull, Temperature-sensitive liposomes for doxorubicin delivery under MRI guidance, J Control Release, 143 (2010) 120-127.
[24] E. Evans, D. Needham, Physical-Properties of Surfactant Bilayer-Membranes - Thermal Transitions, Elasticity, Rigidity, Cohesion, and Colloidal Interactions, J Phys Chem-Us, 91 (1987) 4219-4228.
[25] K. Kono, S. Nakashima, D. Kokuryo, I. Aoki, H. Shimomoto, S. Aoshima, K. Maruyama, E. Yuba, C. Kojima, A. Harada, Y. Ishizaka, Multi-functional liposomes having temperature-triggered release and magnetic resonance imaging for tumor-specific chemotherapy, Biomaterials, 32 (2011) 1387-1395.
[26] M. de Smet, S. Langereis, S. van den Bosch, K. Bitter, N.M. Hijnen, E. Heijman, H. Grull, SPECT/CT imaging of temperature-sensitive liposomes for MR-image guided drug delivery with high intensity focused ultrasound, J Control Release, 169 (2013) 82-90.
[27] B.L. Viglianti, S.A. Abraham, C.R. Michelich, P.S. Yarmolenko, J.R. MacFall, M.B. Bally, M.W. Dewhirst, In vivo monitoring of tissue pharmacokinetics of liposome/drug using MRI: illustration of targeted delivery, Magn Reson Med, 51 (2004) 1153-1162.
[28] M. de Smet, E. Heijman, S. Langereis, N.M. Hijnen, H. Grull, Magnetic resonance imaging of high intensity focused ultrasound mediated drug delivery from temperature-sensitive liposomes: an in vivo proof-of-concept study, J Control Release, 150 (2011) 102-110.
[29] T. Tagami, W.D. Foltz, M.J. Ernsting, C.M. Lee, I.F. Tannock, J.P. May, S.D. Li, MRI monitoring of intratumoral drug delivery and prediction of the therapeutic effect with a multifunctional thermosensitive liposome, Biomaterials, 32 (2011) 6570-6578.
[30] A. Kheirolomoom, C.Y. Lai, S.M. Tam, L.M. Mahakian, E.S. Ingham, K.D. Watson, K.W. Ferrara, Complete regression of local cancer using temperature-sensitive liposomes combined with ultrasound-mediated hyperthermia, J Control Release, 172 (2013) 266-273.
[31] N. Hijnen, E. Kneepkens, M. de Smet, S. Langereis, E. Heijman, H. Grull, Thermal combination therapies for local drug delivery by magnetic resonance-guided high-intensity focused ultrasound, Proc Natl Acad Sci U S A, 114 (2017) E4802-E4811.
[32] H. Grull, S. Langereis, Hyperthermia-triggered drug delivery from temperature-sensitive liposomes using MRI-guided high intensity focused ultrasound, J Control Release, 161 (2012) 317-327.
[33] N. Hijnen, S. Langereis, H. Grull, Magnetic resonance guided high-intensity focused ultrasound for image-guided temperature-induced drug delivery, Adv Drug Deliv Rev, (2014).
[34] N. Kamaly, T. Kalber, A. Ahmad, M.H. Oliver, P.W. So, A.H. Herlihy, J.D. Bell, M.R. Jorgensen, A.D. Miller, Bimodal paramagnetic and fluorescent liposomes for cellular and tumor magnetic resonance imaging, Bioconjug Chem, 19 (2008) 118-129.
[35] N. Kamaly, T. Kalber, G. Kenny, J. Bell, M. Jorgensen, A. Miller, A novel bimodal lipidic contrast agent for cellular labelling and tumour MRI, Org Biomol Chem, 8 (2010) 201-211.
[36] N. Kamaly, T. Kalber, M. Thanou, J.D. Bell, A.D. Miller, Folate receptor targeted bimodal liposomes for tumor magnetic resonance imaging, Bioconjug Chem, 20 (2009) 648-655.

[37] S. Song, D. Liu, J. Peng, H. Deng, Y. Guo, L.X. Xu, A.D. Miller, Y. Xu, Novel peptide ligand directs liposomes toward EGF-R high-expressing cancer cells in vitro and in vivo, Faseb J, 23 (2009) 1396-1404.
[38] A.D. Miller, Lipid-based nanoparticles in cancer diagnosis and therapy, Journal of drug delivery, 2013 (2013) 165981.
[39] A.D. Miller, Delivery of RNAi therapeutics: work in progress, Expert review of medical devices, 10 (2013) 781-811.
[40] A. Haque, M.S. Faizi, J.A. Rather, M.S. Khan, Next generation NIR fluorophores for tumor imaging and fluorescence-guided surgery: A review, Bioorg Med Chem, 25 (2017) 2017-2034.
[41] E.V. Rosca, M. Wright, R. Gonitel, W. Gedroyc, A.D. Miller, M. Thanou, Thermosensitive, near-infrared-labeled nanoparticles for topotecan delivery to tumors, Mol Pharm, 12 (2015) 1335-1346.
[42] D. Needham, J.Y. Park, A.M. Wright, J. Tong, Materials characterization of the low temperature sensitive liposome (LTSL): effects of the lipid composition (lysolipid and DSPE-PEG2000) on the thermal transition and release of doxorubicin, Faraday Discuss, 161 (2013) 515-534; discussion 563-589.
[43] T. Tagami, M.J. Ernsting, S.D. Li, Efficient tumor regression by a single and low dose treatment with a novel and enhanced formulation of thermosensitive liposomal doxorubicin, J Control Release, 152 (2011) 303-309.
[44] C.A. Schneider, W.S. Rasband, K.W. Eliceiri, NIH Image to ImageJ: 25 years of image analysis, Nat Methods, 9 (2012) 671-675.
[45] C.D. Landon, J.Y. Park, D. Needham, M.W. Dewhirst, Nanoscale Drug Delivery and Hyperthermia: The Materials Design and Preclinical and Clinical Testing of Low Temperature-Sensitive Liposomes Used in Combination with Mild Hyperthermia in the Treatment of Local Cancer, Open Nanomed J, 3 (2011) 38-64.
[46] H. Huang, M. Dunne, J. Lo, D.A. Jaffray, C. Allen, Comparison of computed tomography- and optical image-based assessment of liposome distribution, Mol Imaging, 12 (2013) 148-160.
[47] A. Suganami, T. Toyota, S. Okazaki, K. Saito, K. Miyamoto, Y. Akutsu, H. Kawahira, A. Aoki, Y. Muraki, T. Madono, H. Hayashi, H. Matsubara, T. Omatsu, H. Shirasawa, Y. Tamura, Preparation and characterization of phospholipid-conjugated indocyanine green as a near-infrared probe, Bioorg Med Chem Lett, 22 (2012) 7481-7485.
[48] E.E. Paoli, D.E. Kruse, J.W. Seo, H. Zhang, A. Kheirolomoom, K.D. Watson, P. Chiu, H. Stahlberg, K.W. Ferrara, An optical and microPET assessment of thermally-sensitive liposome biodistribution in the Met-1 tumor model: Importance of formulation, J Control Release, 143 (2010) 13-22.
[49] P. Tardi, E. Choice, D. Masin, T. Redelmeier, M. Bally, T.D. Madden, Liposomal encapsulation of topotecan enhances anticancer efficacy in murine and human xenograft models, Cancer Res, 60 (2000) 3389-3393.
[50] K.D. Fugit, B.D. Anderson, The role of pH and ring-opening hydrolysis kinetics on liposomal release of topotecan, J Control Release, 174 (2014) 88-97.
[51] W.C. Zamboni, S. Strychor, E. Joseph, D.R. Walsh, B.A. Zamboni, R.A. Parise, M.E. Tonda, N.Y. Yu, C. Engbers, J.L. Eiseman, Plasma, tumor, and tissue disposition of STEALTH liposomal CKD-602 (S-CKD602) and nonliposomal CKD-602 in mice bearing A375 human melanoma xenografts, Clin Cancer Res, 13 (2007) 7217-7223.
[52] P. Thevenaz, U.E. Ruttimann, M. Unser, A pyramid approach to subpixel registration based on intensity, IEEE Trans Image Process, 7 (1998) 27-41.
[53] G.M. Lanza, C. Moonen, J.R. Baker, Jr., E. Chang, Z. Cheng, P. Grodzinski, K. Ferrara, K. Hynynen, G. Kelloff, Y.E. Lee, A.K. Patri, D. Sept, J.E. Schnitzer, B.J. Wood, M. Zhang, G. Zheng, K. Farahani, Assessing the barriers to image-guided drug delivery, Wiley Interdiscip Rev Nanomed Nanobiotechnol, 6 (2014) 1-14.
[54] T.M. Allen, P.R. Cullis, Liposomal drug delivery systems: from concept to clinical applications, Adv Drug Deliv Rev, 65 (2013) 36-48.

[55] B.M. Dicheva, G.A. Koning, Targeted thermosensitive liposomes: an attractive novel approach for increased drug delivery to solid tumors, Expert Opin Drug Deliv, 11 (2014) 83-100.
[56] L.H. Lindner, H.M. Reinl, M. Schlemmer, R. Stahl, M. Peller, Paramagnetic thermosensitive liposomes for MR-thermometry, Int J Hyperthermia, 21 (2005) 575-588.
[57] M. de Smet, N.M. Hijnen, S. Langereis, A. Elevelt, E. Heijman, L. Dubois, P. Lambin, H. Grull, Magnetic resonance guided high-intensity focused ultrasound mediated hyperthermia improves the intratumoral distribution of temperature-sensitive liposomal doxorubicin, Invest Radiol, 48 (2013) 395-405.
[58] L. Li, T.L. ten Hagen, M. Hossann, R. Suss, G.C. van Rhoon, A.M. Eggermont, D. Haemmerich, G.A. Koning, Mild hyperthermia triggered doxorubicin release from optimized stealth thermosensitive liposomes improves intratumoral drug delivery and efficacy, J Control Release, 168 (2013) 142-150.
[59] M.P. Melancon, A.M. Elliott, A. Shetty, Q. Huang, R.J. Stafford, C. Li, Near-infrared light modulated photothermal effect increases vascular perfusion and enhances polymeric drug delivery, J Control Release, 156 (2011) 265-272.
[60] G. Kong, R.D. Braun, M.W. Dewhirst, Characterization of the effect of hyperthermia on nanoparticle extravasation from tumor vasculature, Cancer Res, 61 (2001) 3027-3032.
[61] G. Kong, R.D. Braun, M.W. Dewhirst, Hyperthermia enables tumor-specific nanoparticle delivery: effect of particle size, Cancer Res, 60 (2000) 4440-4445.
[62] L. Li, T.L. ten Hagen, A. Haeri, T. Soullie, C. Scholten, A.L. Seynhaeve, A.M. Eggermont, G.A. Koning, A novel two-step mild hyperthermia for advanced liposomal chemotherapy, J Control Release, 174 (2014) 202-208.
[63] W.J. Lokerse, M. Bolkestein, T.L. Ten Hagen, M. de Jong, A.M. Eggermont, H. Grull, G.A. Koning, Investigation of Particle Accumulation, Chemosensitivity and Thermosensitivity for Effective Solid Tumor Therapy Using Thermosensitive Liposomes and Hyperthermia, Theranostics, 6 (2016) 1717-1731.
[64] S. Langereis, T. Geelen, H. Grull, G.J. Strijkers, K. Nicolay, Paramagnetic liposomes for molecular MRI and MRI-guided drug delivery, NMR Biomed, 26 (2013) 728-744.
[65] A. de Vries, M.B. Kok, H.M. Sanders, K. Nicolay, G.J. Strijkers, H. Grull, Multimodal liposomes for SPECT/MR imaging as a tool for in situ relaxivity measurements, Contrast Media Mol Imaging, 7 (2012) 68-75.
[66] G.J. Strijkers, W.J. Mulder, R.B. van Heeswijk, P.M. Frederik, P. Bomans, P.C. Magusin, K. Nicolay, Relaxivity of liposomal paramagnetic MRI contrast agents, MAGMA, 18 (2005) 186-192.
[67] N.M. Hijnen, A. Elevelt, J. Pikkemaat, C. Bos, L.W. Bartels, H. Grull, The magnetic susceptibility effect of gadolinium-based contrast agents on PRFS-based MR thermometry during thermal interventions, J Ther Ultrasound, 1 (2013) 8.
[68] N.A. Patankar, D. Waterhouse, D. Strutt, M. Anantha, M.B. Bally, Topophore C: a liposomal nanoparticle formulation of topotecan for treatment of ovarian cancer, Invest New Drugs, 31 (2013) 46-58.
[69] A.W. Wong, B.Z. Fite, Y. Liu, A. Kheirolomoom, J.W. Seo, K.D. Watson, L.M. Mahakian, S.M. Tam, H. Zhang, J. Foiret, A.D. Borowsky, K.W. Ferrara, Ultrasound ablation enhances drug accumulation and survival in mammary carcinoma models, J Clin Invest, 126 (2016) 99-111.

Graphical Abstract